

Aerodynamic Considerations For The Design Of An Experimental Climate Chamber

Frantisek VRANAY¹

Technical University of Kosice,
Faculty of Civil Engineering,
Kosice, Slovakia
Email: frantisek.vranay@tuke.sk

Clayton STONE²

Technical University of Kosice,
Faculty of Civil Engineering,
Kosice, Slovakia
Email: clayton.stone@tuke.sk

Marek KUSNIR³

Technical University of Kosice,
Faculty of Civil Engineering,
Kosice, Slovakia
Email: marek.kusnir@tuke.sk

Jozef Simicek⁴

Technical University of Kosice,
Faculty of Civil Engineering,
Kosice, Slovakia
Email: jozef.simicek@tuke.sk

Abstract— Sustainable building technologies, designed to create an indoor environment that uses fewer resources and generates less waste often rely on piece-meal measurements or computer simulations to predict their efficiency. Measured whole building performance is often limited to a geographic location and weather conditions inhibiting its ability to be repeated. An exponential rise in modern computing has also created a constant need for the verification of individual computer programs. Numerous computational programs such as: FLUENT, CFX / CFD developed by engineers to comfortably solve Computational Fluid Dynamics (CFD) open new possibilities for the simulation of physical phenomena and solution of research tasks. However, a comprehensive test platform for benchmarking has until now not been available to scientists. The paper uses novel software developed by the authors, to mimic static pressure on a test building by ignoring the turbulent behaviour of the air stream for a better understanding of the effects of turbulence. The results calculated in different computational programs can be compared in order to deal with their potential differences and were considered in the construction of a climate chamber at the Technical University of Kosice

Keywords— Navier-Stokes equation; Computational fluid dynamics; Finite element method; Laminar flow; Relative pressure at barrier centre axis; ANSYS-CFX/CFD, SIXIS

I. INTRODUCTION

In smart building design, the building envelope constitutes the boundary, as opposed to the barrier, between the internal and external environments. The building envelope therefore adjusts gains and losses to and from the interior either inherently, through static elements such as building mass or cohesively through automatic response or control. Studying the effects of wind on buildings, a scientific phenomenon known as

aero-elastic instability, is designed to assist engineers in practice. Experimental methods in wind tunnels and "in situ" measurements are often used to analyse the pressure distribution of individual segments that various bodies are subjected to. By this manner, the works of Baines (1), Castro and Robins (2) Sakamoto (3) and others obtained data which were instrumental for numerical analysis. However the benefit of measuring in wind tunnels has its limitations due to Reynolds number to the extent that some authors have preferred to conduct wind measurements in-situ. Known as the measuring cube with dimensions of 6 (m) on each axis, the Silsoe Institute Research UK, was used by Richards, Hoxey and Short (4, 5) to obtain results of pressure distribution on individual surfaces of an enveloped cube and compared them with results obtained by measurement in a wind tunnel. They revealed higher values of monitored variables on the roof and leeward side of the object. For the modelling of flow around objects, methods have recently been developed for computer assisted modelling of flow CFD (Computational Fluid Dynamics). The comparison of numerical mathematics and computer modelling with experimental measurements was dealt with by Wright and Easom (6, 7). Their search for optimal modelling was disseminated in CWE conference proceedings, (8). They observed and modelled the character of flow, pressure distribution, wind speed and temperature around an object and the results were compared with those of existing structures. Generalized gust-front factor framework that captures dynamic features inherent in wind load effects in gust-fronts originating from a downburst/thunderstorm were also researched by D. Kwon and A. Kareem (9). This is akin to the gust loading factor format used in codes and standards world-wide for the treatment of conventional boundary layer winds. Since this paper deals with a multivalent laboratory that constantly monitors the building envelope, building environment, storage devices and service systems using wind, temperature, pressure and heat sensors, consideration was also given to methodology for determining where to install air quality sensors to increase security, (10) .

II. AIR FLOW CONSIDERATIONS

The task of solving fluid flow leads to the formulation of a system of partial differential equations which can be solved approximately using the finite element method (FEM). An independently developed calculation program, SIXIS, calculated the surface pressure of objects subjected to air flow, which, unlike FLUENT, CFX / CFD programs, ignores turbulence. Calculated pressure can therefore be objectively compared to a vertical wall that forms a barrier against air currents and also in the area in which the effects of turbulence are reflected to the smallest degree. A case is considered where the airflow may be modelled using Navier-Stokes equations which govern the flow of a compressible Newtonian fluid, (1). The continuity equation for such a case in vector form can be determined by the following vector notation.

$$\int_V \left(\frac{\partial \rho}{\partial t} + \nabla \cdot (\rho \bar{c}) \right) dV = 0 \quad (1)$$

For the balance of momentum it follows that:

$$\int_V \rho \left(\frac{\partial \bar{c}}{\partial t} + (\bar{c} \cdot \nabla) \bar{c} + \nabla p - \bar{g} \right) dV = \int_V (\eta \Delta \bar{c} + \eta \nabla (\nabla \cdot \bar{c}) + \lambda \nabla (\nabla \cdot \bar{c})) dV. \quad (2)$$

For the balance of energy it follows that:

$$\begin{aligned} \frac{\partial}{\partial t} \int_V e dV + \int_V \nabla e \bar{c} dV + \int_V \nabla p \cdot \bar{c} dV - \int_V \rho \bar{g} \cdot \bar{c} dV + W_Q = \\ = \eta \int_V \left[\Delta \bar{c} + \left(1 + \frac{\lambda}{\eta} \right) \nabla (\nabla \cdot \bar{c}) \right] \cdot \bar{c} dV, \end{aligned} \quad (3)$$

Where:

$\rho = \rho(x, y, z)$ is the density of a mass,

$\bar{c} = \dot{u}(x, y, z, t) \cdot \vec{i} + \dot{v}(x, y, z, t) \cdot \vec{j} + \dot{w}(x, y, z, t) \cdot \vec{k}$ is the velocity field,

$p = p(x, y, z, t)$ is the pressure field,

$\bar{g} = g_x(x, y, z, t) \cdot \vec{i} + g_y(x, y, z, t) \cdot \vec{j} + g_z(x, y, z, t) \cdot \vec{k}$ is the force field,

$\bar{q} = q_x(x, y, z, t) \cdot \vec{i} + q_y(x, y, z, t) \cdot \vec{j} + q_z(x, y, z, t) \cdot \vec{k}$ is the heat flux inside the border of a closed volume,

W_Q is the performance of thermal energy,

E is the conserved energy,

η is the dynamic viscosity of the fluid,

λ is the second coefficient of viscosity,

III. SOLUTION USING FEM

The solutions of such a system of equations are components of a velocity vector and pressure, which can be computed so that a condition resulting from the balance of power can be achieved. For an element with nodes the approximate solution can be described using a linear combination of time and space variables, (11).

$$\begin{aligned} \dot{u} &= \dot{u}(x, y, z, t) = \sum_{i=1}^n \dot{u}_i(t) N_i^v(x, y, z), \\ \dot{v} &= \dot{v}(x, y, z, t) = \sum_{i=1}^n \dot{v}_i(t) N_i^v(x, y, z), \\ \dot{w} &= \dot{w}(x, y, z, t) = \sum_{i=1}^n \dot{w}_i(t) N_i^v(x, y, z), \\ p &= p(x, y, z, t) = \sum_{i=1}^n p_i(t) N_i^p(x, y, z), \end{aligned} \quad (4)$$

Where $1 \leq j \leq n$

Following the introduction of operators $[m]$, $[l(\{\bar{c}\})]$, $[k]$, $[b]$ and $\{g\}$, the following relations may be derived:

$$\begin{aligned} \frac{\partial}{\partial t} [m] \{\bar{c}\} + [l(\{\bar{c}\})] \{\bar{c}\} - [k] \{\bar{c}\} &= \{g\} + [b]^T \{p\}, \\ [b] \{\bar{c}\} &= \{0\} \end{aligned} \quad (5)$$

Such a solution to the i -th node of the e -th finite element is expressed in the form

$$\{\bar{c}\} = \{\bar{c}\}_i^e = \left[\dot{u} \quad \dot{v} \quad \dot{w} \right]_i^e{}^T$$

Over time, the components of the velocity vector function as acceleration

$$\frac{\partial}{\partial t} \{\bar{c}\}_i^e = \left[\frac{\partial \dot{u}}{\partial t} \quad \frac{\partial \dot{v}}{\partial t} \quad \frac{\partial \dot{w}}{\partial t} \right]_i^e{}^T \quad (6)$$

The mass matrix from local elements of acceleration in i -th node of the e -th finite element is expressed as:

$$[m] = [m]_i^e = \begin{bmatrix} m_{11} & m_{12} & m_{13} \\ m_{21} & m_{22} & m_{23} \\ m_{31} & m_{32} & m_{33} \end{bmatrix}_i^e \quad (7)$$

The mass matrix of convective acceleration components in the i -th node of the e -th finite element is expressed as:

$$[l] = [l]_i^e = \begin{bmatrix} \dot{u}_i l_1 & \dot{u}_i l_2 & \dot{u}_i l_3 \\ \dot{v}_i l_1 & \dot{v}_i l_2 & \dot{v}_i l_3 \\ \dot{w}_i l_1 & \dot{w}_i l_2 & \dot{w}_i l_3 \end{bmatrix}_i^e \quad (8)$$

The matrix frictional forces at the i -th node of the e -th finite element is expressed in the form:

$$[k] = [k]_i^e = \begin{bmatrix} k_{11} & k_{12} & k_{13} \\ k_{21} & k_{22} & k_{23} \\ k_{31} & k_{32} & k_{33} \end{bmatrix}_i^e \quad (9)$$

The matrix of continuity at the i -th node of the e -th finite element can be expressed in the form

$$[b] = [b]_i^e = [b_{11} \quad b_{12} \quad b_{13}]_i^e \quad (10)$$

The vector of the external volume of the i -th node of the e -th finite element is expressed as:

$$\{g\} = \{g\}_i^e = \begin{Bmatrix} g_1 \\ g_2 \\ g_3 \end{Bmatrix}_i^e \quad (11)$$

IV. TIME APPROXIMATIONS

When dealing with non-stationary tasks it is also necessary to perform a time approximation after separating spatial and time variables (4). For the flow of an ideal fluid in each time point, the validity of relations is considered (5):

$$[M] \left(\frac{\partial}{\partial t} \{\bar{c}\} \right) + [L(\{\bar{c}\})] \{\bar{c}\} - [K] \{\bar{c}\} = \{\bar{G}\} - [B]^T \{p\}$$

$$[B] \{\bar{c}\} = \{0\}, \quad (12)$$

The validity of relations (12) can be considered at each time step, and also when determining two points in time: $b-1, b$:

$$[M] \{\bar{a}\}_{b-1} + [L(\{\bar{c}\}_{b-1})] \{\bar{c}\}_{b-1} - [K] \{\bar{c}\}_{b-1} = \{\bar{G}\}_{b-1} - [B]^T \{p\}_{b-1},$$

$$[B] \{\bar{c}\}_{b-1} = \{0\},$$

$$[M] \{\bar{a}\}_b + [L(\{\bar{c}\}_b)] \{\bar{c}\}_b - [K] \{\bar{c}\}_b = \{\bar{G}\}_b - [B]^T \{p\}_b,$$

$$[B] \{\bar{c}\}_b = \{0\},$$

$$\Delta \bar{a}_b = \bar{a}_b - \bar{a}_{b-1},$$

$$\Delta p_b = p_b - p_{b-1},$$

$$\Delta \bar{c}_b = \bar{c}_b - \bar{c}_{b-1},$$

$$\Delta \bar{G}_b = \bar{G}_b - \bar{G}_{b-1},$$

$$[M] \{\Delta \bar{a}\}_b + [L(\{\bar{c}\}_b)] \{\Delta \bar{c}\}_b - [K] \{\Delta \bar{c}\}_b = \{\Delta \bar{G}\}_b - [B]^T \{\Delta p\}_b,$$

$$[B] \{\Delta \bar{c}\}_b = \{0\}. \quad (13)$$

After approximating acceleration the following linear function is valid:

$$t = \langle t_b, t_{b+1} \rangle,$$

$$\bar{a}(t) = \bar{a}_{b-1} + \frac{\bar{a}_b - \bar{a}_{b-1}}{t_b - t_{b-1}} t = \bar{a}_{b-1} + \frac{\Delta \bar{a}_b}{\Delta t_b} t,$$

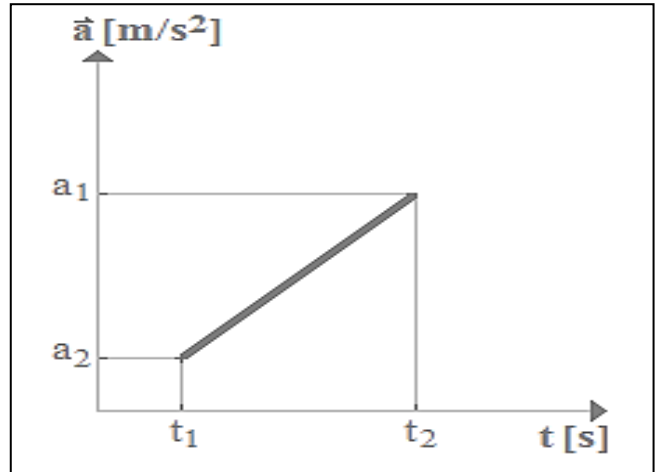


Fig. 1. Time acceleration approximation defined by linear functions

$$\bar{c}(t) = \int_0^{\Delta t} \left(\bar{a}_{b-1} + \frac{\Delta \bar{a}_b}{\Delta t_b} t \right) dt + \bar{c}_{b-1} = \bar{a}_{b-1} t + \Delta \bar{a}_b \frac{t^2}{2 \Delta t_b} + \bar{c}_{b-1}$$

$$\bar{c}_b = \left[\bar{a}_{b-1} t + \Delta \bar{a}_b \frac{t^2}{2 \Delta t_b} \right]_0^{\Delta t} + \bar{c}_{b-1} = \bar{a}_{b-1} \Delta t_b + \Delta \bar{a}_b \frac{\Delta t_b}{2} + \bar{c}_{b-1}$$

$$\Delta \bar{c}_b = \bar{a}_{b-1} \Delta t_b + \Delta \bar{a}_b \frac{\Delta t_b}{2} \Rightarrow \Delta \bar{a}_b = \frac{2}{\Delta t_b} \Delta \bar{c}_b - 2 \bar{a}_{b-1}$$

$$\frac{2}{\Delta t_b} [M] \{\Delta \bar{c}\}_{t=b} + [L(\{\bar{c}\}_{t=b})] \{\Delta \bar{c}\}_{t=b} - [K] \{\Delta \bar{c}\}_{t=b} = \{\Delta G\}_{t=b} - [B]^T \{\Delta p\}_{t=b} + 2 [M] \{\bar{a}\}_{t=b-1}$$

$$[B] \{\Delta \bar{c}\}_{t=b} = \{0\}.$$

$$[K_c]_{t=b} = \frac{2}{\Delta t_b} [M] + [L(\{\bar{c}\}_{t=b})] - [K],$$

$$\{R\}_{t=b} = \{\Delta G\}_{t=b} - [B]^T \{\Delta p\}_{t=b} + 2 [M] \{\bar{a}\}_{t=b-1},$$

$$[K_c]_{t=b} \{\Delta \bar{c}\}_{t=b} = \{R\}_{t=b},$$

$$[B] \{\Delta \bar{c}\}_{t=b} = \{0\},$$

$$\bar{c}_b = \bar{c}_{b-1} + \Delta \bar{c}_b,$$

$$\Delta \bar{a}_b = \frac{2}{\Delta t_b} \Delta \bar{c}_b - 2 \bar{a}_{b-1},$$

$$\bar{a}_b = \bar{a}_{b-1} + \Delta \bar{a}_b. \quad (14)$$

V. LAMINAR FLOWS

Vorticity (turbulence) is considered to be zero for a planar sliding laminar flow of an incompressible fluid.

$$\omega_z(x, y) = \frac{\partial \dot{v}(x, y)}{\partial x} - \frac{\partial \dot{u}(x, y)}{\partial y} = 0. \quad (15)$$

The introduction of a scalar stream function $\Psi(x, y)$, based on the concept of streamlines, can be expressed by the velocity component:

$$\begin{aligned} \dot{u}(x, y) &= \frac{\partial \Psi(x, y)}{\partial y}, \\ \dot{v}(x, y) &= -\frac{\partial \Psi(x, y)}{\partial x}. \end{aligned} \quad (16)$$

By substituting components of speed, derivative functions can be expressed (16) in terms of (non-turbulence) (15); and can be considered a valid equation for determining sliding laminar flow.

$$\omega_z = \frac{\partial \Psi^2}{\partial x^2} + \frac{\partial \Psi^2}{\partial y^2} = 0. \quad (17)$$

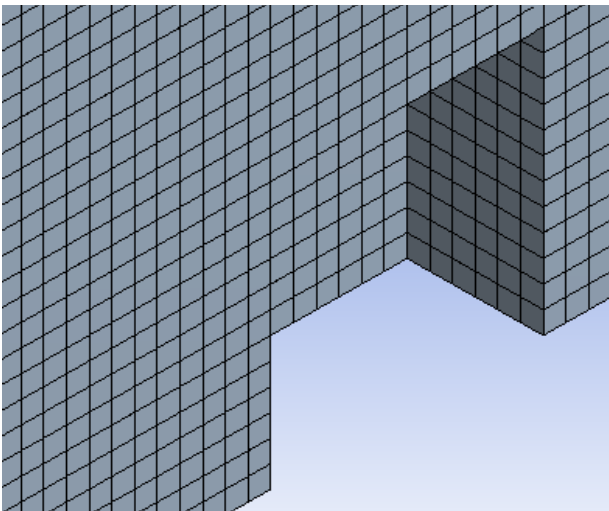


Fig. 2. Finite element mesh in ANSYS / CFX

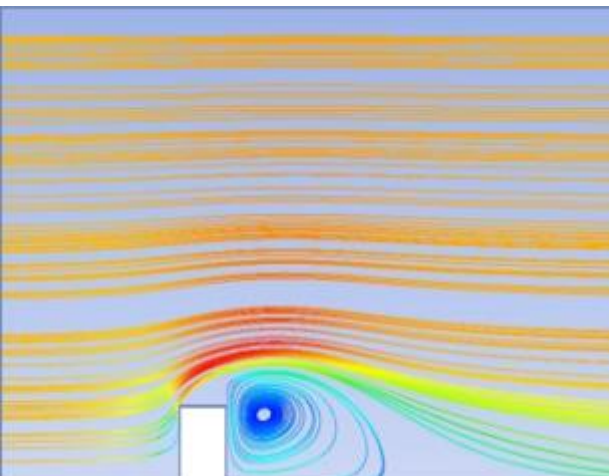


Fig. 3. Flow field ANSYS / CFX

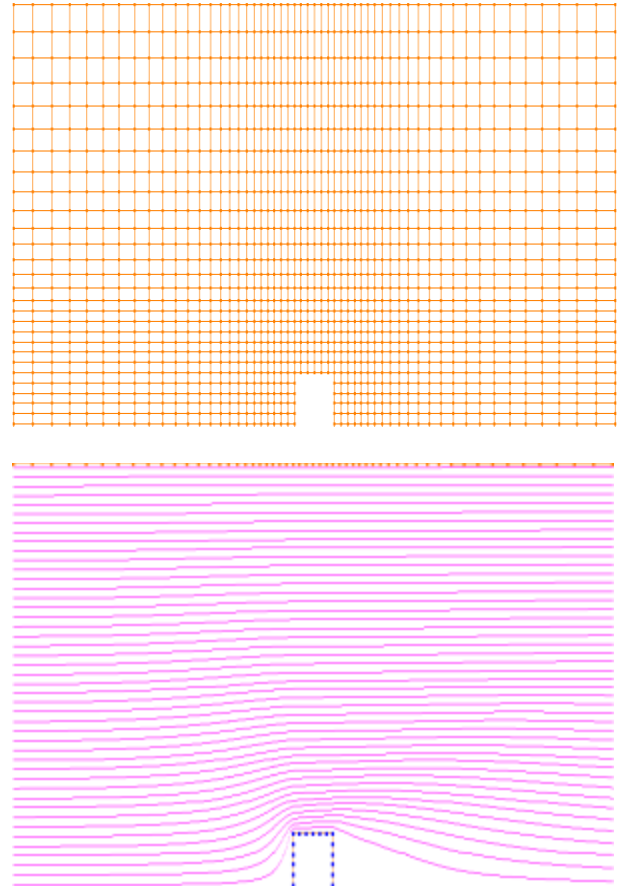


Fig. 4. Top: SIXIS Finite element mesh; Bottom: SIXIS Flow field

VI. EXPRESSION OF PRESSURE IN RELATIVE TERMS

Shape factors are commonly used for the quantitative evaluation of the distribution of applied pressure in construction practice, so that the specific shape of the enveloped body is generally dependent on the shape of the velocity profile of the air flow and the position of the body. The local value for the concept of the constant velocity profile can be expressed using the relationship:

$$C_p = \frac{p(y)}{\frac{1}{2} \rho \dot{u}(y)^2}, \quad (18)$$

Where:

$p(y)$ is the experimental measurement or calculation based on FEM observed local pressure value at height y ,

ρ is the assumed air density,

$\dot{u}(y)$ is the measured horizontal component of wind speed, which is not affected by the barrier corresponding to the measured value of the local pressure $p(y)$.

VII. CONSIDERATIONS APPLICABLE TO THE CALCULATION OF STATIC PRESSURE

The prevention of adverse effects of wind by determining the size and distribution of the pressure field is a significant input factor for the designer. Velocity and pressure field measurements acting on the test building enveloped by an airstream will be obtained by direct measurement using multi-directional thermo-anemometers and wind vanes from Ahlborn. For the numerical solution of equation (13) a pressure field can be estimated from the known velocity field. In general, it is possible to consider the validity of the balance equations for each part of the calculated area (Figure 3), which can be calculated numerically using the finite-element network. The size and shape of the network is directly affected by the size and shape of the building. In symmetric examples, it is possible for the validity of equation (13) to be restricted to the centre line of the building (Figure 4) and thus simplify the numerical model for two-dimensional solutions.

Flow equation (15) is solved only when the trajectories of particles of a fluid or flow field are known. In order to address the current field of equations (15), it can be assumed that the trajectory of an imaginary particle is determined by the terrain and area of buildings exposed to windward effects. After a certain height above the ground an undisturbed horizontal trajectory of flowing air particles (Figure 4) can be considered. Resistive force exerted by an object enveloped with a flow of air can be determined numerically from the assumption that the wind exposed barrier is not entrained in the air stream (20). From operating pressure it is possible to quantify the known nodal values of speed.

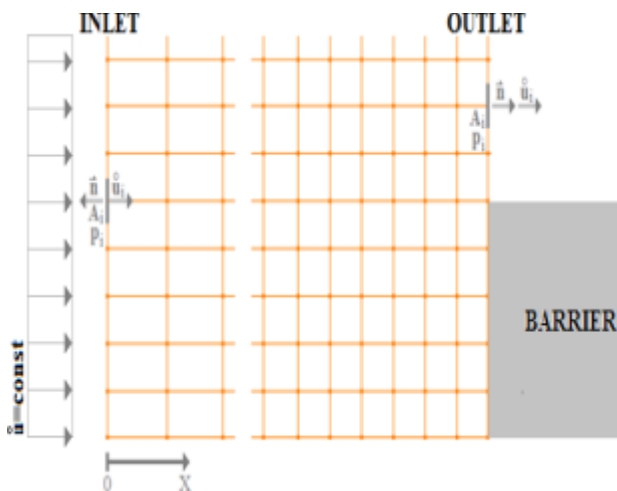


Fig. 5. Oriented flows and their balancing

The pressure in the fluid can be considered as the sum of the static and dynamic components:

$$P = P_s + P_d, \quad (19)$$

Where:

P_s is the static pressure component,

ρ is the air density,

c is the size of this velocity vector.

The dynamic pressure component can be expressed from a known velocity air flow:

$$P_d = -\frac{1}{2} \rho c^2$$

$$\vec{n} \cdot \sum_{Input} ((\rho \dot{u}_i) \dot{u}_i A_i + p_i A_i) +$$

$$\vec{n} \cdot \sum_{Input} ((\rho \dot{u}_i) \dot{u}_i A_i + p_i A_i) = 0 \quad (20)$$

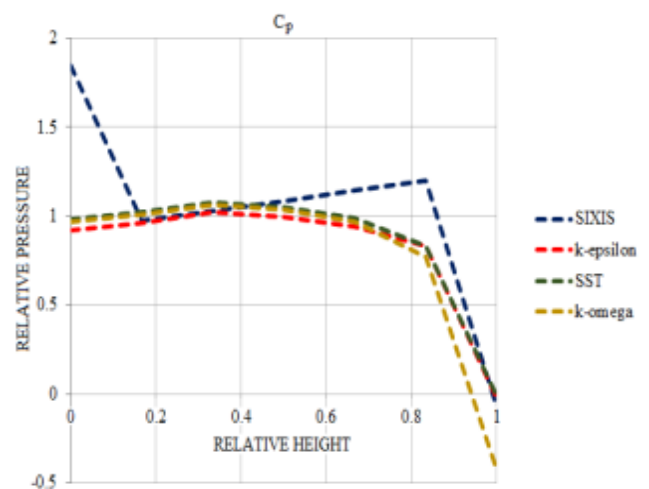


Fig. 6. Pressure propagation through the wall ($s = 24ms^{-1}$, $\rho = 1.25kgm^{-3}$)

These considerations were implemented for efficient and effective dimensioning of the climate chamber which is shown in Figures 7-9



Fig. 7. View of duct-work of climate chamber under construction



Fig.8. View of duct-work of climate chamber under construction

VIII. CONCLUSION

The calculation models which the widely used ANSYS program implements: Model: $k-\epsilon$, SST, $k-\omega$, are turbulent based and assume that part of the kinetic energy of the air stream is transformed as a result of friction, which is reflected by a fall in the rate of pressure and/or velocity. This decrease in the rate of air flow due to friction is attributable to momentum flux. At the point of turbulence, lower calculated pressure values are observed (Figure 6) in model: $k-\epsilon$, and SST, $k-\omega$. In contrast, the SIXIS calculation program ignores the turbulent behaviour of the air stream for a better understanding of the effects of turbulence. The bottom fifth of the wall exhibited a significant difference between the models, where SIXIS shows the highest values for turbulence of all the programs. Significant friction air flow also occurs at the corners of the enveloped barriers. In addition, the upper part revealed a difference in results between the turbulent model from program CFX / CFD and SIXIS. The differences of the calculated results between this newly developed program together with ANSYS makes it possible to notice the places where turbulence occurs to a greater extent which would not be possible using ANSYS alone. This model and its details are representative of the current state of the art trends in building construction. Special consideration was taken to reduce the effects of thermal bridges and maximize airtightness. The model within the climate chamber is a 'smart building' designed to identify the number of occupants their location and level of activity via CO_2 consumption and motion sensors. The practical implications of the applied research and development of intelligent building service systems is the creation of a platform to research the efficiency and interoperability of components and renewable energy technologies which will be based on experimental analysis.

ACKNOWLEDGMENT

This paper was supported by the operational program project: Research and Development project: Centrum VUKONZE, with code ITMS: 26220220064, co-financed by from resources of the European Regional Development Fund.

REFERENCES

- [1] W. D. BAINES, "Effect of velocity distribution on wind loads on a tall building," University of Toronto, TP 6203, 1962.
- [2] I.P. CASTRO, A.G. ROBINS, "The flow around a surface-mounted cube in uniform and turbulent streams," Journal of Fluid Mechanics, Vol. 79, part 2, 1977.
- [3] H. SAKAMOTO, M. ARIE, "Flow around a cubic body immersed in turbulent Boundary Layer", 1982.
- [4] P.J. RICHARDS, R.P. HOXLEY, L.J. SHORT, "Wind pressures on a 6 m cube", Journal of Wind Engineering and Industrial Aerodynamics, 89 pp. 1553-1564, 2001.
- [5] P.J. RICHARDS, R.P. HOXLEY, L.J. SHORT, "A 6 m cube in an atmospheric boundary layer flow. Part 1. Full-scale and wind tunnel results", Wind and Structures, Vol. 5, No. 2-4 pp.165-176, 2002.
- [6] N.G. WRIGHT, G.J. EASOM, "Comparison of several computational turbulence models with full – scale measurements of flow around a building", Wind and Structures, Vol.2, No. 4, pp. 305-323, 1999.
- [7] EASOM, G.J.: Improved turbulence models for computational wind engineering", PhD. Thesis in Civil Engineering, The University of Nottingham, UK, 2000.
- [8] G KNAPP, N.WRIGHT, J OWEN, "Comparison of full scale and CFD results for the Silsoe 6m cube", Proceedings of the 11th International Conference on Wind Engineering, June, Lubbock, TX, Vol.1, pp. 163-170, 2003.
- [9] D. Kwon, A. Kareem, "Generalized gust-front factor: A computational framework for wind load effects", Engineering Structures, 2012
- [10] D.G. Eliades, M.P. Michaelides, C.G. Panayiotou M.M. Polycarpou, "Security orientated sensor placement in intelligent buildings", Building and Environment , 2013.
- [11] O.C ZIENKIEWICZ, "Comparison of several computational turbulence models with full – scale measurements of flow around a building", Wind and Structures, Vol.2, No. 4, pp. 305-323, 1999.